LATTICE PINNING OF MAGNETIC DOMAINS IN THE HELIMAGNET $Ba_2CuGe_2O_7$

J. CHOVAN, N. PAPANICOLAOU

University of Crete and Research Center of Crete
(Heraklion 71003, Greece; e-mail: papanico@physics.uoc.gr)

UDC 53.183

The layered magnetic compound $Ba_2CuGe_2O_7$ exhibits spiral antiferromagnetic order thanks to a Dzyaloshinskii—Moriya (DM) anisotropy that is allowed by crystal symmetry. Here, we theoretically examine some finer issues such as the experimentally observed lattice pinning of the propagation vector of helical magnetic domains along the crystallographic (1,1,0) or $(1,\bar{1},0)$ direction. We find that the DM anisotropy alone would actually lead to pinning along the (1,0,0) or (0,1,0) direction, but the agreement with experiment is restored upon including an additional exchange anisotropy that is also consistent with symmetry. The present results also shed light on the so-called bisection rule which has been abstracted from experiment in presence of an in-plane magnetic field.

$Ba_2CuGe_2O_7$ is an essentially two-dimensional spin system that exhibits the spiral antiferromagnetic order due to the Dzyaloshinskii—Moriya (DM) anisotropy [1, 2]. A series of experiments, including standard magnetometry, elastic, and inelastic neutron scattering [3—7], has established that the ground state is an incommensurate spiral with period (pitch) $L \approx 37$ lattice units (219 Å) at zero external magnetic field. When a field of strength H is applied along the c-axis, the period $L = L(H)$ grows to infinity at $H_c \approx 2$ T and the ground state degenerates into a commensurate spin-flop state for $H > H_c$. Thus, one obtained the first experimental realization of the incommensurate-to-commensurate (IC) phase transition whose gross features were theoretically predicted some time ago in [8].

$Ba_2CuGe_2O_7$ is an insulator and its magnetic properties may be understood in terms of localized spins. Crystal symmetry provides the necessary input for the construction of a discrete Heisenberg Hamiltonian, but a theoretical analysis is greatly facilitated by the continuum approximation which leads to a certain effective field theory that is a variant of the relativistic nonlinear σ model. The continuum approximation is justified by the fact that the anisotropy is sufficiently weak and thus leads to the ground state which is a spiral with a reasonably large period. Hence, the nonlinear σ model may be safely employed for the study of ground-state properties and the corresponding low-energy dynamics. The resulting theoretical picture was found to be in general agreement with experiment [3—7] and further clarified the precise nature of the Dzyaloshinskii-type IC transition [9, 10]. Yet, discreteness effects are important to understand some finer issues of experimental interest and are the main focus of the present paper.

The unit cell of $Ba_2CuGe_2O_7$ is partially illustrated in Fig. 1, where we display only the magnetic Cu^{2+} ions with spin $s = 1/2$. The lattice constants are $a = b = 8.466$ Å and $c = 5.445$ Å. Since Cu atoms form a perfect square lattice within each layer, it is also useful to consider the orthogonal axes x, y, and z obtained from the conventional crystal axes a, b, and c by a 45° azimuthal rotation. The major spin interaction between nearest in-plane neighbors along the x or y axis is antiferromagnetic, while the interaction between the nearest out-of-plane neighbors along the z axis is ferromagnetic and rather weak [3]. Therefore, we are effectively dealing with a 2D antiferromagnet defined on a square lattice with natural axes x and y and lattice constant $d = a/\sqrt{2} = 5.986$ Å.

Hence, in the first approximation, the spin dynamics is described in terms of a 2D isotropic Heisenberg model. However, because of the low tetragonal symmetry of this crystal (space group $P\bar{4}2_1m$), the effective Heisenberg Hamiltonian may contain an interesting combination of antisymmetric (DM) and symmetric exchange anisotropies. In the following, anisotropy is introduced in steps of increasing complexity, invoking the results of a complete symmetry analysis [9, 10] as they become necessary.

Experiments were initially [3—6] analyzed in terms of a relatively simple extension of the isotropic Heisenberg model defined by the Hamiltonian

$$W = \sum_{\langle \mathbf{r}\mathbf{r}' \rangle} \left[J \left(\mathbf{S}_{\mathbf{r}} \cdot \mathbf{S}_{\mathbf{r}'} \right) + \mathbf{D}_{\mathbf{r}\mathbf{r}'} \cdot \left(\mathbf{S}_{\mathbf{r}} \times \mathbf{S}_{\mathbf{r}'} \right) \right], \qquad (1)$$

where the sum extends over all bonds $\langle \mathbf{r}\mathbf{r}' \rangle$ connecting any two neighboring sites $\mathbf{r}$ and $\mathbf{r}'$ on a square lattice. Symmetry requires that the exchange constant J be the same for all bonds, while the constant vectors $\mathbf{D}_{\mathbf{r}\mathbf{r}'}$

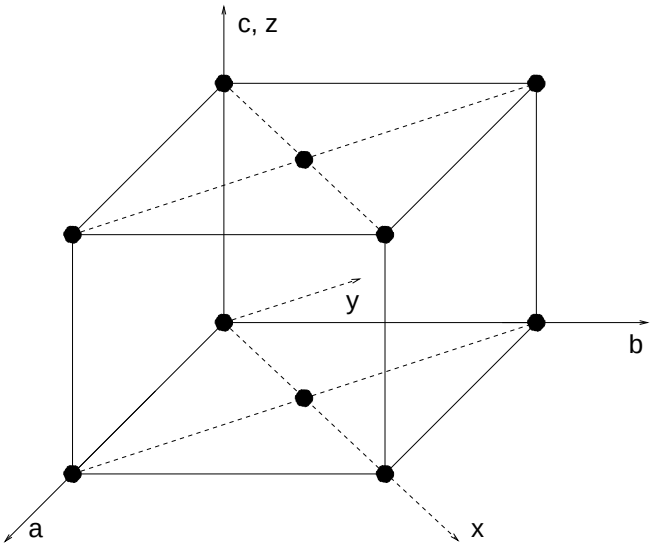

Fig. 1. Partial illustration of the unit cell of $Ba_2CuGe_2O_7$ displaying only the magnetic Cu^{2+} ions, denoted by solid circles, which form a perfect square lattice within each layer

which account for the pure DM anisotropy are of the form

$$\mathbf{D}_{\mathbf{rr}'} = (0, D_\perp, \pm D_z) \ \text{ for bonds along } \ x,$$

$$\mathbf{D}_{\mathbf{rr}'} = (D_\perp, 0, \pm D_z) \ \text{ for bonds along } \ y, \qquad (2)$$

where Cartesian components are taken along the axes x, y, and z of Fig. 1, and a sign alternation at consecutive bonds is present in the third component $\pm D_z$. In fact, all available experimental evidence suggests that $D_z \ll D_\perp$ in $Ba_2CuGe_2O_7$. Therefore, while possible implications of a finite D_z are studied in [9, 10], we set $D_z = 0$ throughout the present paper. Hamiltonian (1) is then written in a completely explicit form as

$$W = \sum\nolimits_{mn} [\, J\, \mathbf{S}_{m,n} \cdot (\mathbf{S}_{m+1,n} + \mathbf{S}_{m,n+1}) +$$

$$+ D_\perp \left(S^z_{m,n} S^x_{m+1,n} - S^x_{m,n} S^z_{m+1,n}\right) +$$

$$+ D_\perp \left(S^y_{m,n} S^z_{m,n+1} - S^z_{m,n} S^y_{m,n+1}\right)], \qquad (3)$$

where m and n are integers that advance along the x and y axes of the square lattice and $\mathbf{S}_{m,n} = (S^x_{m,n}, S^y_{m,n}, S^z_{m,n})$ is the spin operator at site (m, n). At this point, we invoke the classical approximation whereby spin operators are treated as classical vectors with magnitude $\mathbf{S}^2_{m,n} = s^2$. The ground state is then described by the classical spin configuration that minimizes Hamiltonian (3). To search for a minimum, we employ the spherical parametrization

$$S^x_{m,n} = s\,(-1)^{m+n} \sin\Theta_{m,n} \cos\Phi_{m,n}\,,$$

$$S^y_{m,n} = s\,(-1)^{m+n} \sin\Theta_{m,n} \sin\Phi_{m,n}\,,$$

$$S^z_{m,n} = s\,(-1)^{m+n} \cos\Theta_{m,n}\,, \qquad (4)$$

where the staggering factor $(-1)^{m+n}$ reflects the antiferromagnetic nature of the basic exchange interaction. Inserting Eq. (4) in Eq. (3) yields an energy functional whose variation leads to a coupled system of nonlinear equations for the angular variables $\Theta_{m,n}$ and $\Phi_{m,n}$. We shall not write out these equations explicitly, but merely state a class of analytical spiral-like solutions

$$\Theta_{m,n} = m\,\gamma_1 + n\,\gamma_2, \qquad \Phi_{m,n} = -\psi, \qquad (5)$$

where the *constants* γ_1, γ_2, and ψ are constrained only by the curious relation

$$\tan\psi = \frac{\sin\gamma_2}{\sin\gamma_1}. \qquad (6)$$

The corresponding energy per unit cell is given by

$$w = s^2 J[\, 2 - \cos\gamma_1 - \cos\gamma_2 -$$

$$-\varepsilon\,(\sin\gamma_1 \cos\psi + \sin\gamma_2 \sin\psi)\,] \qquad (7)$$

where the trivial constant $2s^2 J$ amounts to removing the energy of the pure Néel state, and

$$\varepsilon = D_\perp / J \qquad (8)$$

is a dimensionless anisotropy constant whose magnitude is left arbitrary for the moment.

The helical spin configurations constructed above are stationary points of the energy functional for any choice of the constants γ_1, γ_2, and ψ that satisfy constraint (6). However, the absolute minimum of the energy is achieved for the specific choice $\gamma_1 = \gamma_2 = \arctan(\varepsilon/\sqrt{2})$ and $\psi = \pi/4$, or

$$\Theta_{m,n} = (m+n)\arctan(\varepsilon/\sqrt{2}), \quad \Phi_{m,n} = -\pi/4\,,$$

$$w = 2s^2 J\left[1 - \sqrt{1 + \varepsilon^2/2}\right] =$$

$$= \varepsilon^2 s^2 J \left(-\frac{1}{2} + \frac{\varepsilon^2}{16} + \ldots\right), \qquad (9)$$

which is a screw-type spiral whose propagation vector points along the crystalographic $b = (0, 1, 0)$ axis, while the spin rotates in a plane perpendicular to the same axis. An equivalent solution that propagates along the

$a = (1,0,0)$ axis is also possible but will not be given a further consideration.

The preceding result is already contradicted by the experimental fact that the spiral propagates along the $x = (1,1,0)$ or the $y = (1,\bar{1},0)$ axis [3—7]. To make this fact completely explicit, we consider a special member of the family solutions (5) obtained by setting $\psi = 0$, and thus $\gamma_2 = 0$ by virtue of constraint (6), while the remaining constant γ_1 is chosen to minimize the reduced energy $w = s^2 J(1 - \cos\gamma_1 - \varepsilon \sin\gamma_1)$ to yield $\gamma_1 = \arctan(\varepsilon)$ and

$$\Theta_{m,n} = m \arctan(\varepsilon), \qquad \Phi_{m,n} = 0\,,$$

$$w = s^2 J\left[1 - \sqrt{1+\varepsilon^2}\right] = \varepsilon^2 s^2 J\left(-\frac{1}{2} + \frac{\varepsilon^2}{8} + ...\right), \quad (10)$$

which is a spiral that propagates along the x axis while the spin rotates within the xz plane. Both of these facts are consistent with experiment, but the spiral energy given by Eq. (10) is *larger* than the energy of a screw-type spiral given by Eq. (9) to within terms of order ε^4. In other words, the pure DM Hamiltonian (3) cannot explain the observed pinning of the propagation vector of the spiral along the x or y axis.

Before discussing a resolution of this apparent discrepancy, it is instructive to view the analytical solutions given by Eqs. (5)–(7) from a slightly different perspective.Thus, we attempt to first minimize energy (7) at a fixed angle ψ, with γ_1 and γ_2 related by constraint (6). The result of this minimization is written here in a perturbative form as

$$\sin\gamma_1 = \varepsilon\cos\psi\left[1 - \frac{1}{2}\left(\cos^4\psi + \sin^4\psi\right)\varepsilon^2 + ...\right],$$

$$\sin\gamma_2 = \varepsilon\sin\psi\left[1 - \frac{1}{2}\left(\cos^4\psi + \sin^4\psi\right)\varepsilon^2 + ...\right], \quad (11)$$

and the corresponding energy per unit cell is given by

$$w = \varepsilon^2 s^2 J\Big\{-\frac{1}{2} + \frac{1}{32}\left[3 + \cos(4\psi)\right]\varepsilon^2 + ...\Big\}. \quad (12)$$

This result is consistent with Eqs. (9) and (10), for $\psi = \pi/4$ and $\psi = 0$, respectively, and reinforces our earlier conclusion that the absolute minimum of the energy is achieved for $\psi = \pi/4$ which leads to the screw-type spiral of Eq. (9).

For a sufficiently weak anisotropy ($\varepsilon \ll 1$), Eq. (11) may be further approximated by $\gamma_1 \approx \varepsilon\cos\psi$ and $\gamma_2 \approx \varepsilon\sin\psi$ which are inserted in Eq. (5) to yield

$$\Theta_{m,n} \approx \varepsilon\left(m\cos\psi + n\sin\psi\right), \quad \Phi_{m,n} = -\psi. \quad (13)$$

This is a class of degenerate helical configurations with common energy $w \approx -\varepsilon^2 s^2 J/2$ which is independent of angle ψ. Eq. (13) describes a helix that propagates along the x' axis of Fig. 2, which forms an angle ψ with respect to the x axis, while the spin rotates in the $x''z$ plane whose intersection with the basal plane forms an angle $-\psi$ with respect to the x axis. The angle formed by the normal to the spin plane (axis y'') and the spiral propagation vector (axis x') is bisected by the conventional crystal axis $b = (0,1,0)$. Therefore, in the leading $\varepsilon \ll 1$ approximation, the theory predicts that spirals may propagate in an arbitrary direction (angle ψ) as long as they conform with the "bisection rule" just described.

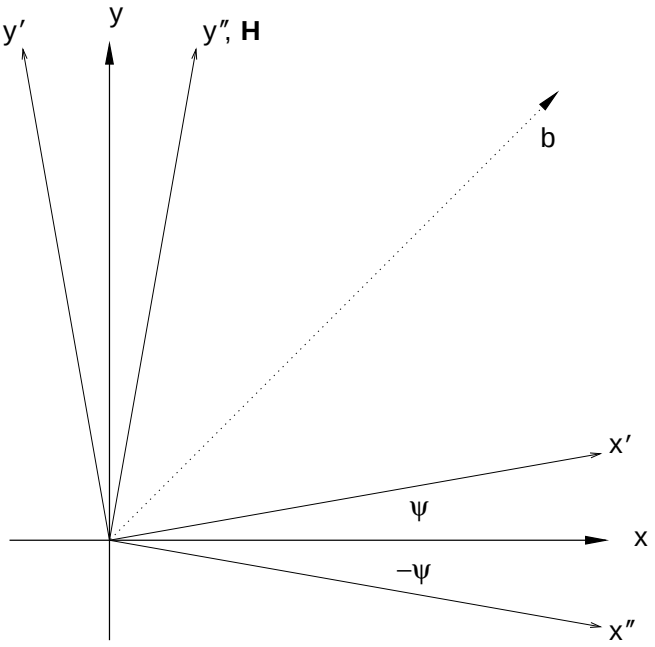

Fig. 2. Illustration of the ideal bisection rule. The spiral propagation vector points along the x' axis, while the spin rotates within the $x''z$ plane. This ideal rule is experimentally realized when a sufficiently strong in-plane magnetic field **H** is applied along the y'' axis

However, when the terms of order ε^4 are included in the energy, as in Eq. (12), a screw-type spiral propagating along the a or b axis ($\psi = \pm\pi/4$) is predicted to be energetically favorable. As mentioned already, this prediction is contradicted by experiment where spirals always propagate along the x or y axis ($\psi = 0$ or $\pi/2$) in the absence of an in-plane external magnetic field. Therefore, the pure DM anisotropy included in Hamiltonian (1) needs to be ammended.

A more general type of anisotropy is suggested in [11] and [12—14] which is usually referred to as the KSEA anisotropy. The latter was already invoked in [7, 9, 10] to explain the observed distortion of the spiral from its ideal sinusoidal shape, as well as the structure of the magnon spectrum determined via inelastic neutron scattering. In the continuation of this paper, we show that the KSEA anisotropy also explains (a) the observed lattice pinning of the spiral propagation vector along the $x = (1, 1, 0)$ or $y = (1, \bar{1}, 0)$ direction in the absence of an in-plane field, and (b) a remnant of the bisection rule observed via neutron diffraction in the presence of an in-plane field [5].

The KSEA extension of Hamiltonian (3) reads

$$W = \sum_{mn} \Big[J_1 S^x_{m,n} S^x_{m+1,n} + J_2 S^y_{m,n} S^y_{m+1,n} +$$

$$+ J_3 S^z_{m,n} S^z_{m+1,n} + J_2 S^x_{m,n} S^x_{m,n+1} + J_1 S^y_{m,n} S^y_{m,n+1} +$$

$$+ J_3 S^z_{m,n} S^z_{m,n+1} + D_\perp \big(S^z_{m,n} S^x_{m+1,n} - S^x_{m,n} S^z_{m+1,n} +$$

$$+ S^y_{m,n} S^z_{m,n+1} - S^z_{m,n} S^y_{m,n+1} \big) \Big], \qquad (14)$$

where

$$J_1 = J - \Delta, \qquad J_2 = J + \Delta, \qquad J_3 = J - \Delta \qquad (15)$$

and

$$\Delta = \frac{D_\perp^2}{4J} = \frac{1}{4} \varepsilon^2 J. \qquad (16)$$

One should keep in mind that Hamiltonian (14) is still consistent with the underlying space group $P\bar{4}2_1m$ but is not the most general Hamiltonian allowed by symmetry [9, 10]. Nevertheless, Eq. (14) has been the starting point for a reasonably successful analysis of a vast set of experimental data and will be adopted here without further questioning.

Our aim is then to find the classical minima of Hamiltonian (14). One may again employ the spherical parametrization (4), but the resulting coupled equations for $\Theta_{m,n}$ and $\Phi_{m,n}$ do not seem to admit an analytical solution (when $\Delta \neq 0$) of the type obtained earlier in Eqs. (5)—(7) within the pure DM model ($\Delta = 0$). Instead, our strategy is to derive a perturbative expansion for small values of $\varepsilon = D_\perp / J$ of practical interest.

To leading order in ε, the ground state may be obtained by minimizing a suitable continuum energy functional [7, 9, 10]. The resulting spiral generalizes Eq. (13) to the extent that anharmonic distortions occur in the profile of the angular variable $\Theta_{m,n}$ which is no longer a linear function of $\varepsilon(m \cos\psi + n \sin\psi) \approx (x \cos\psi + y \sin\psi)$. Instead, the complete solution may be written as

$$\Theta_{m,n} \approx \theta \left(x \cos\psi + y \sin\psi \right), \qquad \Phi_{m,n} = -\psi, \qquad (17)$$

where ψ is an arbitrary constant angle and $\theta(u)$ is a function of $u = x \cos\psi + y \sin\psi$ that may be expressed in terms of an elliptic integral. This family of solutions is degenerate in the sense that the energy is independent of the angle ψ. As a consequence, the bisection rule summarized in Fig. 2 remains valid in the presence of the KSEA anisotropy to the leading order in ε.

However, the above degeneracy is again broken beyond the leading approximation. To demonstrate this fact, we have systematically carried out the continuum expansion beyond the leading approximation. Technical details are too cumbersome to be described here in any detail, but the main conclusion may be stated by quoting the final result for the ground-state energy per unit cell calculated to order ε^4:

$$w = \varepsilon^2 s^2 J \Big\{ -\frac{1}{2} \delta^2 + \left[C_0 + C_1 \cos\left(4\psi\right) \right] \varepsilon^2 + ... \Big\}. \qquad (18)$$

When this procedure is applied to the pure DM model ($\Delta = 0$) we find that $\delta^2 = 1$, $C_0 = 3/32$, and $C_1 = 1/32$, which agree with the results of Eq. (12) and thus provide an important check of consistency. In the presence of the KSEA anisotropy ($\Delta = \varepsilon^2 J/4$), we find

$$\delta^2 = 0.53189772\,,$$

$$C_0 = 0.00098724, \qquad C_1 = -0.00474723, \qquad (19)$$

obtained by the numerical calculation of a large number of elliptic-type integrals. The most important feature of Eq. (19) is that the constant C_1 is now negative and thus leads to the minimum energy in Eq. (18) for $\psi = 0$ or $\pi/2$; i.e., for a spiral that propagates along the x or y axis, in agreement with experiment.

The strength of anisotropy appropriate for the description of $Ba_2CuGe_2O_7$ is estimated from the value of the spiral pitch measured at zero field [7] to be $\varepsilon = D_\perp / J \approx 0.18$. Therefore, anisotropy appears to be sufficiently weak for the validity of the leading-order continuum approximation. For instance, the relative correction induced by the second-order term in Eq. (18) is of the order of 5×10^{-4}. Nevertheless, such a tiny correction is important for explaining the correct lattice pinning of a spiral propagation vector along the x or y axis, as well as some measurable deviations from the ideal bisection rule summarized in Fig. 2.

The bisection rule was initially discovered through neutron diffraction [5] in the presence of an in-plane magnetic field

$$\mathbf{H} = (\cos\chi, \sin\chi, 0)\, H \tag{20}$$

which forms an angle χ with respect to the x axis. The spiral was then observed to adjust its propagation vector according to the rule

$$\chi + \psi = \frac{\pi}{2}, \tag{21}$$

in order to minimize the Zeeman energy induced by the magnetic field. Returning to Fig. 2, a spiral that initially propagates along the x axis ($\psi = 0$) is reoriented to propagate along the x' axis ($\psi \neq 0$) so that the normal to the spin plane (axis y'') points along the applied magnetic field.

Actually, the above rule was observed only for sufficiently strong fields $H > 0.5$ T. For weak fields, a reorientation of the spin structure to conform with the ideal bisection rule is inhibited by a small tetragonal anisotropy that is present in the second-order term of Eq. (18). The appropriate modification of Eq. (21) is then derived by an argument similar to that given in [5], now taking into account the theoretical prediction for the tetragonal anisotropy contained in Eq. (18):

$$H^2 = \frac{8A\,\sin(4\psi)}{\sin 2(\psi+\chi)}, \tag{22}$$

where

$$A = \left(\frac{2sJ}{g_{ab}\,\mu_{\rm B}}\right)^2 \frac{2\,|C_1|\,\varepsilon^4}{\langle \sin^2\theta \rangle} \tag{23}$$

is a numerical factor which is here calculated in terms of the constant C_1 of Eq. (19), the average $\langle \sin^2\theta \rangle = 0.56517$ taken over a period of the spiral profile of Eq. (17), and some basic parameters determined by independent experiments [3—7]; namely, the spin value $s = 1/2$, the exchange constant $J = 0.96$ meV, the DM anisotropy $\varepsilon = D_\perp/J = 0.1774$, the gyromagnetic ratio $g_{ab} = 2.044$ for a field applied in some direction within the basal plane, and the Bohr magneton $\mu_{\rm B}$.

Putting everything together, we find that $A = 1.1 \times 10^{-3}$ T^2. The corresponding predictions

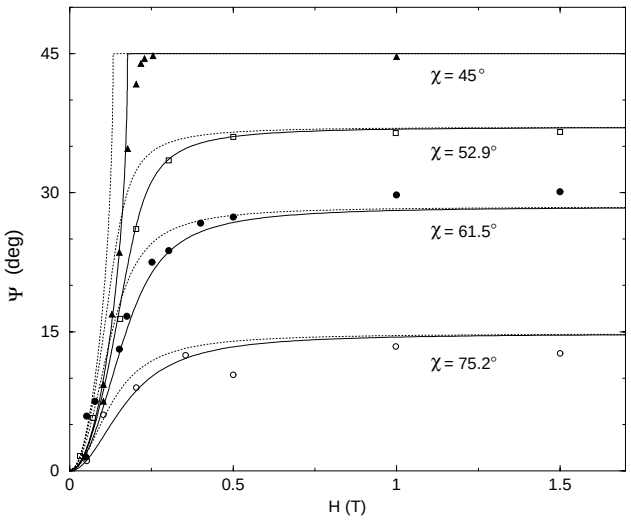

Fig. 3. Deviations from the ideal bisection rule predicted by Eq.(22) applied for $A = 1.1 \times 10^{-3}$ T^2 (dotted lines) and $A = 1.95 \times 10^{-3}$ T^2 (solid lines). Note that the ideal bisection rule ($\chi + \psi = \pi/2$) is indeed realized for a sufficiently strong in-plane magnetic field $H > 0.5$ T. Experimental data denoted by symbols were extracted from Fig. 3 in [5]

of Eq. (22) are depicted by dotted lines in Fig. 3, where we display the direction of the spiral propagation (angle ψ) as a function of applied field (H) for various field orientations (angle χ). The ideal bisection rule of Eq. (21) is clearly reproduced for sufficiently strong fields ($H > 0.5$ T) but measurable deviations occur for weak fields. Altogether, our theoretical predictions are in reasonable agreement with experiment. A better fit is obtained by treating the constant A in Eq. (22) as an adjustable phenomenological parameter determined by a global fit of the experimental data, as was originally done in [5] to obtain $A = 1.95 \times 10^{-3}$ T^2. The corresponding predictions of Eq. (22) are also depicted in Fig. 3 (solid lines) and provide an improved overall fit of the data.

To summarize, the KSEA extension of the pure DM anisotropy is capable of explaining a large set of data pertaining to the IC phase transition observed in $Ba_2CuGe_2O_7$, as well as some finer issues such as the lattice pinning of helical magnetic domains. One should keep in mind that DM+KSEA is not the most general type of anisotropy allowed by symmetry [7, 9, 10]. In this respect, we mention here that a significant departure from KSEA seems to occur in the layered antiferromagnet $K_2V_3O_8$. The space group of this compound is different ($P4bm$) but leads to a Heisenberg Hamiltonian that is very similar to

the one encountered in $Ba_2CuGe_2O_7$. However, the experimental investigation [15] of $K_2V_3O_8$ revealed the occurrence of interesting spin-flop and spin-reorientation transitions but provided no evidence for incommensurate magnetism. A preliminary theoretical analysis [15, 16] concluded that $K_2V_3O_8$ is characterized by an easy-axis anisotropy, which is impossible to occur in the KSEA limit [10].

This paper is dedicated to our friend Professor Victor G. Bar′yakhtar on the occasion of his 75th birthday — helimagnetism has been one of the many subjects of interest during his long and fruitful career [17].

1. *Dzyaloshinskii I. E.* // Sov. Phys. JETP. — 1957. — **5**, N 6. — P. 1259—1272.
2. *Moriya T.* // Phys. Rev. — 1960. — **120**, N 1. — P. 91—98.
3. *Zheludev A., Shirane G., Sasago Y. et al.* // Phys. Rev. B — 1996. — **54**, N 21. — P. 15163—15170.
4. *Zheludev A., Maslov S., Shirane G. et al.* // Phys. Rev. Lett. — 1997. — **78**, N 25. — P. 4857—4860.
5. *Zheludev A., Maslov S., Shirane G. et al.* // Phys. Rev. B — 1997. — **56**, N 21. — P. 14006—14012.
6. *Zheludev A., Maslov S., Shirane G. et al.* // Ibid. — 1998. — **57**, N 5. — P. 2968—2978.
7. *Zheludev A., Maslov S., Shirane G. et al.* // Ibid. — 1999. — **59**, N 17. — P. 11432—11444.
8. *Dzyaloshinskii I. E.* // Sov. Phys. JETP — 1964. — **19**, N 4. — P. 960—971; 1965. — **20**, N 1. — P. 223—231; N 3. — P. 665—671.
9. *Chovan J., Papanicolaou N., Komineas S.* // Phys. Rev. B.— 2002. — **65**, N 6. — P. 064433(15).
10. *Chovan J., Papanicolaou N.* Frontiers in Magnetic Materials/ Ed. by An. V. Narlikar. — Berlin: Springer, in press.
11. *Kaplan T. A.* // Z. Phys. B — 1983. — **49**, N 4. — P. 313—317.
12. *Shekhtman L., Entin-Wohlman O., Aharony A.* // Phys. Rev. Lett. — 1992. — **69**, N 5. — P. 836—839.
13. *Shekhtman L., Aharony A., Entin-Wohlman O.* // Phys. Rev. B — 1993. — **47**, N 1. — P. 174—182.
14. *Yildirim T., Harris A. B., Aharony A., Entin-Wohlman O.* //Ibid. — 1995. — **52**, N 14. — P. 10239—10267.
15. *Lumsden M. D., Sales B. C., Mandrus D. et al.* // Phys. Rev. Lett. — 2001. — **86**, N 1. — P. 159—162.
16. *Bogdanov A., Roessler U. K., Wolf M., Müller K.-H.* // Phys. Rev. B — 2002. — **66**, N 21. — P. 214410(16).
17. *Bar'yakhtar V. G., Stefanovskii E. D.* // Sov. Phys. Solid State. — 1970. — **11**, N 7. — P. 1566—1570.

ГРАТКОВИЙ ПІНИНГ МАГНІТНИХ ДОМЕНІВ У МАГНЕТИКУ З ГЕЛІКОЇДАЛЬНОЮ СТРУКТУРОЮ $Ba_2CuGe_2O_7$

Я. Хован, Н. Папаніколау

Р е з ю м е

У шаруватій магнітній сполуці $Ba_2CuGe_2O_7$ реалізується гелікоїдальний магнітний порядок завдяки анізотропії Дзялошинського—Морія (ДМ), яка дозволена симетрією кристала. У роботі теоретично обґрунтовано ряд тонких ефектів, таких, як виявлений експериментально пінінг вектора трансляції магнітних доменів вздовж кристалографічних напрямків (1,1,1) та (1,$\bar{1}$,0). Знайдено, що сама лише ДМ-анізотропія може описати пінінг тільки вздовж напрямків (1,0,0) або (0,1,0), але узгодження з експериментом можна досягти лише з врахуванням додаткової анізотропії обмінного характеру, яка також сумісна із симетрією задачі. Наведені результати до того ж кидають світло на так зване правило розділення, виведене з результатів експерименту з наявністю магнітного поля, прикладеного в площині шарів.

РЕШЕТОЧНЫЙ ПИННИНГ МАГНИТНЫХ ДОМЕНОВ В МАГНЕТИКЕ С ГЕЛИКОИДАЛЬНОЙ СТРУКТУРОЙ $Ba_2CuGe_2O_7$

Я. Хован, Н. Папаниколау

Р е з ю м е

В слоистом магнитном соединении $Ba_2CuGe_2O_7$ реализуется геликоидальный магнитный порядок благодаря анизотропии Дзялошинского—Мория (ДМ), которая разрешена симметрией кристалла. Здесь теоретически обосновывается ряд тонких эффектов, таких, как обнаруженный экспериментально пиннинг вектора трансляции геликоидальных магнитных доменов вдоль кристаллографических направлений (1,1,1) и (1,$\bar{1}$,0). Мы обнаружили, что ДМ-анизотропия сама по себе может описать пиннинг только вдоль направлений (1,0,0) или (0,1,0), но согласие с экспериментом достигается только при учете дополнительной анизотропии обменного характера, которая также совместима с симметрией задачи. Представленные результаты к тому же проливают свет на так называемое правило разделения, выведенное из результатов эксперимента в присутствии магнитного поля, приложенного в плоскости слоев.